TITLE:

Arabidopsis thaliana subclass I ACTIN DEPOLYMERIZING FACTORs regulate nuclear organization and gene expression

AUTHORS:

[1]Tomoko Matsumoto, [2,3]Takumi Higaki, [4]Hirotomo Takatsuka[†], [5]Natsumaro Kutsuna, [1]Yoshiyuki Ogata, [6]Seiichiro Hasezawa, [4]Masaaki Umeda and [1]Noriko Inada*

ADDRESS:

[1]Graduate School of Agriculture, Osaka Metropolitan University, 1-1 Gakuen-cho, Naka-ku, Sakai, Osaka 599-8531, Japan

[2]Graduate School of Science and Technology, Kumamoto University, Kumamoto 860-8555, Japan

[3]International Research Organization for Advanced Science and Technology (IROAST), Kumamoto University, Kumamoto 860-8555, Japan

[4]Graduate School of Science and Technology, Nara Institute of Science and Technology, Takayama-cho 8916-5 Ikoma, Nara 630-0192 Japan

[5]LPIXEL, Inc., 1-6-1 Otemachi, Chiyoda-ku, Tokyo 100-0004, Japan

[6]Graduate School of Science and Engineering, Hosei University, Tokyo 102-8160, Japan

[†]Present address:School of Biological Science and Technology, College of Science and Engineering, Kanazawa University, Kakuma-machi, Kanazawa 920-1192, Japan

*Author in correspondence

ABSTRACT

ACTIN DEPOLYMERIZING FACTOR (ADF) is a conserved protein that regulates the organization and dynamics of actin microfilaments. Eleven ADFs in the *Arabidopsis thaliana* genome are grouped into four subclasses, and subclass I ADFs, ADF1–4, are all expressed throughout the plant. Previously, we showed that subclass I ADFs function in the regulation of the response against powdery mildew fungus as well as in the regulation of cell size and endoreplication. Here, we report a new role of subclass I ADFs in the regulation of nuclear organization and gene expression. Through a microscopic observation of epidermal cells in mature leaves, we found that the size of chromocenters in both *adf4* and transgenic lines where expression of subclass I *ADF*s are downregulated (*ADF1-4Ri*) was reduced compared with that of wild-type Col-0. *A. thaliana* possesses eight *ACTIN* genes, among which *ACT2*, *-7*, and *-8* are expressed in vegetative organs. The chromocenter size in *act7*, but not in the *act2/8* double mutant, was enlarged compared with that in Col-0. Microarray analysis revealed that 1,818 genes were differentially expressed in *adf4* and *ADF1-4Ri*. In particular, expression of 22 nucleotide-binding leucine-rich repeat (*NLR*) genes, which are involved in effector-triggered plant immunity, was reduced in *adf4* and *ADF1-4Ri*. qRT-PCR confirmed the altered expressions shown with microarray analysis. Overall, these results suggest that ADF regulates various aspects of plant physiology through its role in regulation of nuclear organization and gene expression. The mechanism how ADF and ACTIN regulate nuclear organization and gene expression is discussed.

INTRODUCTION

ACTIN DEPOLYMERIZING FACTOR (ADF) is an ancient protein that is conserved among eukaryotes. ADF regulates both the organization and dynamics of actin microfilaments (AFs) by severing and depolymerizing them at the minus end (Inada, 2017). Analyses using various plants including *Arabidopsis thaliana* have revealed that ADFs function in regulating many aspects of plant physiology, including growth and development (Dong et al. 2001, Henty et al. 2011, Inada et al. 2021), flowering (Dong et al. 2001, Burgos-Rivera et al. 2008), immunity against bacterial (Tian et al. 2009, Porter et al. 2012) and fungal pathogens (Inada et al. 2016, Zhang et al. 2017, Sun et al. 2021), root-knot nematodes (Clément et al. 2009), and aphids (Mondal et al. 2018), rhizobial infection and nodule formation (Ortega-Ortega et al. 2020), and responses against drought (Qian et al. 2019, Sengupta et al. 2019), salt stress (Sengupta et al. 2019, Wang et al. 2021), and low temperature (Xu et al. 2021). However, it is unknown how ADFs regulate these broad aspects of plant physiology.

AFs mainly function underneath the plasma membrane by regulating intercellular transport (Henty-Ridilla et al. 2013); however, recent research using animal and insect cells has shown the roles of actin and actin-binding proteins in the nucleus and in the regulation of gene expression.

68 The actin monomer has been shown to be a functional component of RNA polymerases and
69 chromosome remodeling complex (Percipalle and Vartiainen 2019). Furthermore, recent
70 development of nuclear AF visualization method revealed that nuclear AFs are transiently
71 formed upon various stimuli, such as treatments with serum and reagents that induce DNA
72 damage (Baarlink et al. 2013, Hurst et al. 2019) and contribute to the regulation of gene
73 expression (Percipalle and Vartiainen 2019). Cytoplasmic AFs also regulate gene expression by
74 associating with chromatin through nuclear envelope-embedded protein complexes and nuclear
75 lamina (Davidson and Cadot 2021).
76 Interest has increased in plants in the role of actin and actin-binding proteins in the nucleus
77 and in the regulation of gene expression (Porter and Day 2013, Porter and Day 2016, Inada
78 2017). Immunostaining using antibodies that label *A. thaliana* ACTIN2/8 (ACT2/8) and ACT7
79 showed accumulation of these actins within isolated nuclei (Kandasamy et al. 2010). Among the
80 11 members of ADFs in *A. thaliana* (Ruzicka et al. 2007, Inada, 2017), a knockout mutant of
81 *ADF4* showed an increased susceptibility against the bacterial pathogen *Pseudomonas syringae*
82 DC3000 harboring AvrPphB (Tian et al. 2009). This increased susceptibility is correlated with a
83 decreased expression of Flg22-Induced Receptor Kinase 1 (*FRK1*) and Resistance to
84 *Pseuromonas syringae* 5 (*RPS5*), which encode bacterial flagellin-induced receptor kinase and a
85 resistance protein required for recognition of AvrPphB, respectively (Porter et al. 2012). The loss
86 of *A. thaliana ADF9* expression causes reduced expression of *FLOWERING LOCUS C* (*FLC*),
87 which is a master repressor of the transition from the vegetative to reproductive growth, and
88 increased expression of *CONSTANS* (*CO*), *FLOWERING LOCUS T* (*FT*), *SUPRESSOR OF*
89 *CONSTANS1* (*SOC1*), and *LEAFY* (*LFY*), resulting in early flowering (Burgos-Rivera et al.
90 2008).
91 We previously demonstrated that *A. thaliana* subclass I ADFs (ADF1-4), particularly
92 ADF4, are involved in response against powdery mildew fungus (Inada et al. 2016) as well as in
93 the regulation of endoreplication and plant size (Inada et al. 2021) and suggested that subclass I
94 ADFs may have a function in the nucleus and in the regulation of gene expression. The *ADF4*
95 knockout mutant showed strong resistance against the *A. thaliana*-adapted powdery mildew
96 fungus *Golovinomyces orontii*. This resistance was further enhanced in transgenic plants where
97 expression of all subclass I *ADF*s was suppressed (*ADF1-4Ri*). By visualizing AFs with
98 expression of GFP-hTalin (Takemoto et al. 2003), we found that the density and level of
99 bundling of AFs at the cell surface are not significantly altered in both *adf4* and *ADF1-4Ri*.
100 Observation of *adf4* plants expressing ADF4-GFP revealed nuclear localization of ADF4 in
101 addition to colocalization with AFs at the cell surface. Expression of ADF4-GFP complemented
102 the *adf4 G. orontii*-resistant phenotype. However, expression of ADF4-GFP conjugated with
103 nuclear exporting signal did not complement *adf4*, indicating that nuclear localization of ADF4
104 is important for response against *G. orontii* (Inada et al. 2016). We found that *adf4* and *ADF1-*
105 *4Ri* had an increased plant size and an enhanced endoreplication (Inada et al. 2021). All known
106 factors that regulate endoreplication are localized to the nucleus (discussed in Inada et al. 2021),

107 further suggesting the role of subclass I ADFs in the nucleus or in the regulation of events
108 occurring within the nucleus.
109 In this study, we characterized the nuclear morphology and gene expression profile of *A.*
110 *thaliana adf4* and *ADF1-4Ri*. Nuclei in epidermal cells of *A. thaliana* mature leaves contain
111 distinctive chromocenters that are strongly stained with DNA-binding fluorescent dyes (Fransz et
112 al. 2002). By a close observation using confocal laser scanning microscope, we found that the
113 size of these chromocenters of nuclei in the epidermal cells of mature leaves was significantly
114 reduced in *adf4* and *ADF1-4Ri*. The *A. thaliana* genome contains eight ACTIN members, of
115 which *ACTIN2*, -*7*, and -*8* are expressed in vegetative tissues (McKinney and Meagher 1998).
116 We found that *act7*, but not *act2/8* mutants showed increased chromocenter size. Microarray
117 analysis of wild-type Col-0, *adf4*, and *ADF1-4Ri* mature leaves showed that expression of a large
118 number of genes was altered in both *adf4* and *ADF1-4Ri*. These results suggest that actin and
119 ADF are involved in the regulation of nuclear organization and of gene expression.
120
121
122 **RESULTS**
123
124 **The nuclear organization was altered in both *adf4* and *ADF1-4Ri***
125 For the first step to understand the role of ADFs in the nucleus or in the regulation of events
126 occurring in the nucleus, we took a close observation of nuclei using a confocal laser scanning
127 microscope. In fixed-*A. thaliana* mature leaves, 4′,6-diamidino-2-phenylindole (DAPI)-stained
128 nuclei contain well-defined chromocenters (Fransz et al. 2002). These chromocenters consist of
129 heterochromatin regions including centromeric and pericentromeric domains as well as nucleolar
130 organizing regions (NORs) that are composed of ribosomal DNA tandem repeats located in the
131 short arms of chromosomes 2 and 4 (Fransz et al. 2002). NORs are located close to the nucleolus
132 while centromeres are located near the nuclear periphery. By observing epidermal nuclei in
133 mature leaves, we noticed that chromocenters in both *adf4* and *ADF1-4Ri* were smaller than
134 those in Col-0 (Figs. 1A–C). No significant alteration in the shape and size of nuclei was noticed.
135 To quantify the size of chromocenters, maximum projection images produced from Z-stack
136 DAPI-stained nuclei images were processed to evaluate the chromocenter regions. The number
137 of chromocenters per nucleus (Fig. 1D), average size of nucleus (Fig. 1E), average size of
138 chromocenters (Fig. 1F), and percentage of area occupied by chromocenters in the nucleus (Fig.
139 1G) were determined. Wild-type Col-0 nuclei contain 8–10 chromocenters as in previous
140 observations (Fransz et al. 2002). As shown in Fig. 1D, the number of chromocenters per nucleus
141 was unaltered in *adf4* and *ADF1-4Ri*. The size of nuclei in *adf4* and *ADF1-4Ri* was comparable
142 with that in Col-0 (Fig. 1E). However, the average size of chromocenters in both *adf4* and
143 *ADF1-4Ri* was significantly reduced compared with that in Col-0 (Fig. 1F). The percentage of
144 chromocenter occupancy in the nucleus was also significantly reduced in *ADF1-4Ri* but not in
145 *adf4* (Fig. 1G). In *ADF1-4Ri*, expression of all of four subclass I *ADF*s is suppressed by
146 expression of RNAi construct targeting *ADF1* through *ADF4* (Tian et al. 2009). Four

147 independent lines have been established for *ADF1-4Ri* (Tian et al. 2009), and all *ADF1-4Ri* lines
148 showed significant reduction in chromocenter size (Fig. S1). μ
149 Close examination of the obtained images showed that the NOR chromocenters tended to
150 be larger than those near the nuclear periphery in *adf4* and *ADF1-4Ri* (Figs. 1A–C; nucleoli are
151 indicated by dotted lines). We examined the size of NOR chromocenters separately from
152 chromocenters located at the nuclear periphery. The size of chromocenters at the nuclear
153 periphery was significantly reduced in both *adf4* and *ADF1-4Ri* compared with the size of those
154 in Col-0 (Fig. 1H). However, the NOR chromocenter size was not significantly altered in *adf4*
155 compared with that in Col-0, whereas a significant reduction in chromocenter size was observed
156 in *ADF1-4Ri* (Fig. 1I). This result suggests that chromocenters near the nucleoli are affected
157 differently from those near the nuclear periphery in *adf4* and *ADF1-4Ri*.
158 Subclass I *ADF*s are more strongly expressed in mature leaves than in cotyledons (Ruzicka
159 et al. 2007). We examined the chromocenter size of both cotyledons and mature leaves (first
160 leaves) to understand the relationship between loss of subclass I *ADF* expression and
161 chromocenter size reduction. The chromocenter size in the cotyledons of *adf4* and *ADF1-4Ri*
162 was comparable to that in wild-type Col-0 (Figs. 2A–D), whereas the size of chromocenters in
163 the first leaves of *ADF1-4Ri* was significantly reduced (Figs. 2E–H). qRT-PCR confirmed the
164 reduction in expression of all of subclass I *ADF*s in the first leaves (Fig. S2). On the other hand,
165 the level of expression suppression in cotyledons varies among members of subclass I *ADF*s.
166 While *ADF1* and *ADF2*, which showed higher expression in cotyledons compared to first leaves
167 in our growth condition, were suppressed in *ADF1-4Ri* as in first leaves (Figs. S2A and S2B),
168 the expression of *ADF3* and *ADF4*, which was very low in Col-0 cotyledons, was increased in
169 *ADF1-4Ri* cotyledons (Figs. S2C and S2D). Those results may suggest that members of subclass
170 I *ADF*s differently contribute to regulation of chromocenter size.
171 The reduction in chromocenter size could be caused by the decondensation of
172 chromocenters. We performed in situ fluorescence hybridization (FISH) using a probe
173 specifically labeling centromeric repetitive DNA to examine this possibility. Although most
174 FISH labeling showed a condensed pattern, several nuclei showed diffused FISH labeling (Fig.
175 S3), suggesting that the diffusion of heterochromatin caused a reduction in chromocenter size in
176 *adf4* and *ADF1-4Ri*.
177 We also noticed that a portion of the nuclei in *ADF1-4Ri* contained chromocenters that
178 tended to be clustered compared with the relatively random distribution in Col-0 nuclei (Figs.
179 S4A and S4B). We quantified this chromocenter organization by measuring the distance of the
180 two chromocenters (Fig. S4C). The median value of the distances between any closest
181 chromocenter of nuclei was lower in *ADF1-4Ri* than that in Col-0. As the number of
182 chromocenters per nucleus was unaltered in *ADF1-4Ri,* the positioning of chromocenters of
183 *ADF1-4Ri* was disturbed and more aggregated than that in Col-0.
184 Thus, nuclear organization was altered in both *adf4* and *ADF1-4Ri* but more significantly
185 in *ADF1-4Ri*.
186

187 **The size of chromocenters was altered in *act7* but not in *act2/8***
188 Among the 10 *ACT* genes in the *A. thaliana* genome (McDowell et al. 1996a), *ACT2*, *-7*, and *-8*
189 are expressed in the vegetative tissues (An et al. 1996, McDowell et al. 1996b), where subclass I
190 *ADF*s are mainly expressed (Ruzicka et al. 2007). ACT2 and ACT8 are highly similar in amino
191 acid sequences and are functionally equivalent (Kandasamy et al. 2009). We reasoned that if
192 ADFs regulate nuclear organization via AFs, it is possible that *act* mutants also show alterations
193 in nuclear organization. We therefore examined the nuclear morphology of the *act2-1*/*act8-2*
194 double mutant (*act2/8*) as well as that of *act7-4* single mutant (*act7*)(Figs. 3A–C).
195 No significant alterations were observed in the number of chromocenters per nucleus (Fig. 3D)
196 or in the nuclear size (Fig. 3E) in *act2*/*8* or *act7*. We noticed that the size of chromocenters
197 tended to be larger in *act7* (Fig. 3C) than that in Col-0 (Fig. 3A). However, quantitative analysis
198 of chromocenter size showed no significant difference among Col-0, *act2/8*, and *act7* when all
199 chromocenters were included for analysis (Fig. 3F). The percentage of area occupied by
200 chromocenters in the nucleus was also unaltered in *act2/8* and *act7* (Fig. 3G). When
201 chromocenters at the nuclear periphery and those near the nucleolus were separately analyzed,
202 the chromocenters at the nuclear periphery were significantly larger in *act7* than those in Col-0
203 (Fig. 3H), whereas the chromocenters near the nucleolus were comparable among Col-0, *act2/8*,
204 and *act7* (Fig. 3I).These results further confirmed that actin disturbance affects the size of
205 chromocenters, and that chromocenters near the nucleolus were regulated differently from those
206 at the nuclear periphery.
207 We then analyzed chromocenters in *fiz1*, dominant negative mutant of *ACT8*. In *fiz1*
208 homozygous mutant, the organization of AFs is significantly disrupted, and AFs became shorter
209 and thicker comparing to wild type or *fiz1* heterozygous mutant (Kato et al. 2010). As shown in
210 Fig. S5, there was no difference in number of chromocenters per nucleus, nuclear size, and
211 chromocenter size between wild type Col-0 and *fiz1* homozygous mutant.
212
213 **Gene expression profile was significantly altered in both *adf4* and *ADF1-4Ri***
214 The altered nuclear organization in *adf4* and *ADF1-4Ri* described above may affect gene
215 expression. To test this idea, we performed a large-scale gene expression analysis using the
216 Arabidopsis Gene 1.0 ST array. RNA extracted from mature leaves of 4-week-old Col-0, *adf4*,
217 and *ADF1-4Ri* was used for microarray analysis. Two independent sets of plants were used for
218 microarray analysis for biological replication. Genes that showed more than two-fold differences
219 in expression levels in both data set were extracted. With this criterion, we found that expression
220 of 911 genes in total was upregulated in *adf4* and *ADF1-4Ri*, and that of 907 genes in total was
221 downregulated in *adf4* and *ADF1-4Ri* (Figs. 4A and 4B). Among these, expression of 137 genes
222 was upregulated in both *adf4* and *ADF1-4Ri*, whereas that of 232 genes was downregulated in
223 both *adf4* and *ADF1-4Ri* (Tables S1 and S2).
224 Gene Ontology analysis performed for these up- or downregulated genes in both *adf4* and
225 *ADF1-4Ri* revealed enrichment of biotic-responsive genes (Fig. 4C). We also found that
226 downregulated genes included many nucleotide-binding-leucine-rich repeat (*NLR*) genes (Table

227 S3). NLRs function in the recognition of pathogen effectors that are delivered into plant cells.
228 Recognition of effectors by NLRs triggers plant immunity (Pok Man Ngou et al. 2022).
229 Misregulation of *NLR* expression can cause autoimmunity and growth defects, and the
230 expression level of *NLR* genes is therefore maintained at a low level in uninfected plants (Fick et
231 al. 2022). We found that the expression of 22 *NLR* genes were further downregulated in both
232 *adf4* and *ADF1-4Ri* (Table S3). The list of downregulated *NLR*s in both *adf4* and *ADF1-4Ri*
233 included *RPS5* (At1g12220), whose expression is reported to be downregulated in *adf4* (Porter et
234 al. 2012). The expression of five *NLR*s were downregulated in *adf4* but not in *ADF1-4Ri*.
235 Twenty-one *NLR*s showed reduced expression in *ADF1-4Ri* but not in *adf4* (Table S3).
236 Upregulated *NLRs* included one *NLR* in *adf4*, and eight *NLR*s in *ADF1-4Ri*. No *NLRs* were
237 upregulated in both *adf4* and *ADF1-4Ri* (Table S3). This result suggests that each member of
238 subclass I ADFs contributes differently to the regulation of expression of different *NLR*s.
239
240 **qRT-PCR confirmed the altered gene expression in *adf4* and *ADF1-4Ri***
241 As we only took biological duplications for microarray analysis, we verified the microarray data
242 by performing qRT-PCR for genes that are up- or downregulated in both *adf4* and *ADF1-4Ri* by
243 using *ACT8* as an internal control. We selected genes for qRT-PCR analysis based on three
244 criteria: genes whose functions have been reported; genes where the expression level is
245 sufficiently high in Col-0 (based on eFP browser analysis;
246 http://bar.utoronto.ca/efp2/Arabidopsis/Arabidopsis_eFPBrowser2.html), and genes that possess
247 specific sequences that have low homology with other genes.
248 For upregulated genes, At1g13210, At1g18710, At1g45145, At1g52000, At1g52400, and
249 At3g45860 were selected. At1g13210 encodes autoinhibited Ca^{2+}/ATPase II (ACA.l), which
250 functions as a P4-type ATPase that maintains asymmetry between the intra- and extracellular
251 lipid layers in phospholipid membrane bilayers (Axelsen et al. 2001). At1g18710 encodes MYB
252 DOMAIN PROTEIN 47 (MYB47), a member of R2R3-MYB proteins that function in plant
253 primary and secondary metabolism, cell fate determination, development, and responses to both
254 biotic and abiotic stresses (Dubos et al. 2010). *MYB47* expression is reported to be induced by
255 wounding and methyl jasmonate (MeJA) treatment (Devoto et al. 2005). At1g45145 encodes
256 thioredoxin *h5* (TRX5), a member of *h*-type thioredoxin. *A. thaliana TRX5* is required for the
257 response to victorin, an effector produced by a fungus *Cochliobolus victoriae*, which causes
258 Victoria blight of oats (Sweat and Wolpert. 2007). At1g52000, encoding a member of jacalin-
259 related lectin family (Eggermont et al. 2017), is reportedly upregulated by treatment with both
260 jasmonic acid and MeJA (Sasaki-Sekimoto et al., 2005) as well as by inoculation with fungal
261 pathogen *Fusarium oxysporum* (Zhu et al. 2013). At1g52400 encodes BETA GLUCOSIDASE
262 18 (BGLU18), a protein that localizes the endoplasmic reticulum (ER) and accumulates in ER
263 bodies (Ogasawara et al. 2009). BGLU18 is also known to mediate hydrolysis of abscisic acid
264 (ABA)-glucose ester to produce active ABA (Han et al. 2020). At3g45860 encodes CYSTEINE-
265 RICH RECEPTOR-LIKE PROTEIN KINASE 4 (CRK4). *CRK4* expression is induced by
266 salicylic acid treatment and *P. syringae* pv. tomato DC3000 (*Pst*) infection (Chen et al. 2004).

267 Overexpression of *CRK4* induces hypersensitive cell death (Chen et al. 2004) and confers
268 resistance to the virulent bacteria *Pst* (Yeh et al. 2015). *CRK4* overexpression can enhance
269 drought tolerance (Lu et al. 2016). The upregulation of expression of these genes in *adf4* and
270 *ADF1-4Ri* was confirmed with qRT-PCR (Figs. 5A–F).
271 For downregulated genes, At1g58602, At1g58848, At1g61300, At2g05070, At2g05540,
272 and At3g26380 were examined for their expression with qRT-PCR. At1g58602, At1g58848, and
273 At1g61300 encode NLRs. NLRs can be divided into three groups according to their N-terminal
274 domains, namely, those with Toll/interleukin-1 receptor (TIR) domain, coiled-coil (CC) domain
275 (CNL), and RESISTANCE TO POWDERY MILDEW (RPW) 8-like CC domain (Pok Man
276 Ngou et al. 2022). At1g58602, At1g58848, and At1g61300 are all CNL. At1g58602 encodes
277 RPP7 (for resistance to *Peronospora paracitica* 7), which is required for resistance against
278 oomycete *Hyaloperonospora paracitica* Hiks1 (McDowell et al. 2000). The expression of
279 At1g58602, At1g58848, and At1g61300 in wild-type Col-0 was low but detectable (Figs. 5G–I).
280 However, in *adf4* and *ADF1-4Ri*, the expression of these *NLRs* was reduced to an undetectable
281 level (Figs. 5G–I), confirming the microarray results.
282 At2g05070 encodes light-harvesting chlorophyll-binding 2.2 (Lhcb2.2). *Lhcb1*, *Lhcb2*, and
283 *Lhcb3* genes encode polypeptides for trimeric LHCII (Jansson 1999). Lhcb1 is the most
284 abundant among these Lhcb proteins, and Lhcb2 plays a critical role in state transitions
285 (Pietrzykowska et al. 2014). Three genes in *A. thaliana* Col-0 encode *Lhcb2*, namely, *Lhcb2.1*
286 (At2g05100), *Lhcb2.2* (At2g05070), and *Lhcb2.3* (At3g27690). As *Lhcb2.1*, *2.2*, and *2.3* encode
287 identical proteins (Jansson 1999), we designed primers that detect the 3'-UTR of *Lhcb2.2* that
288 showed a decrease in *Lhcb2.2* expression in both *adf4* and *ADF1-4Ri* (Fig. 5J). The expression of
289 *Lhcb2.1* (At2g05100) and *Lhcb2.3* (At3g27690) also exhibited a degree of decrease in
290 expression according to microarray analysis (Table S4). At2g05540 encodes a member of
291 glycine-rich protein family, although the function is largely unknown. Expression of At2g05540
292 is regulated by SWI/SNF chromatin remodeling protein AtCHR12 (Mlynárová et al. 2007) and
293 by the SET domain protein, SDG4, which maintains the level of histone H3 lysine 4 (H3K4) and
294 H3K36 methylation (Cartagena et al. 2008). At3g26380 encodes β-$_L$-ARAPASE (APSE) that
295 functions in the hydrolysis of β-$_L$-arabinopyranosyl residues in arabinogalactan-proteins. A
296 mutation in APSE causes inhibition of the elongation growth of hypocotyls (Imaizumi et al.
297 2017). The expression of both At2g05540 and At3g26380 was reduced in *adf4* and *ADF1-4Ri*
298 (Figs. 5K and 5L). qRT-PCR using *UBQ11* as an internal control confirmed changes in
299 expression of At1g18710, At3g45860, At1g58602 and At2g05070 in *adf4* and *ADF1-4Ri*
300 (Fig.S6).
301 Overall, qRT-PCR analyses confirmed the microarray results, and we concluded that
302 expression of many genes, including those encoding *NLR*s, was significantly altered in *adf4* and
303 *ADF1-4Ri*.
304
305
306 **DISCUSSION**

307
308 Herein, we showed that chromocenter organization was significantly altered in both *adf4* and
309 *ADF1-4Ri*. The size of DAPI-stained chromocenters was significantly reduced in both *adf4* and
310 *ADF1-4Ri*, and part of nuclei in *ADF1-4Ri* showed clustered chromocenters. This reduction in
311 size was likely caused by the decondensation of chromocenters. In the *act7* mutant but not the
312 *act2/8* mutant, the size of chromocenters was increased compared with that of Col-0. Microarray
313 analyses revealed alterations in the expression of many genes in *adf4* and *ADF1-4Ri*. Overall,
314 our results indicate that subclass I ADFs and ACT function in the regulation of nuclear
315 organization and gene expression.
316 Based on previous research using mammalian cells, we propose three possible mechanisms
317 of ADF and ACT regulating nuclear organization and gene expression. First possibility is that
318 ACT monomer in the nucleus regulate chromatin organization and gene expression. In mouse
319 embryonic fibroblasts, loss of β-actin showed an increase in nuclear area and a decrease in DAPI
320 fluorescence intensity in nuclei (Xie et al. 2018). Both immunofluorescence microscopy and
321 western blotting showed that the amount of histone H3 trimethylated at lysine 9 (H3K9me3), a
322 marker of facultative heterochromatin, was increased in β-actin knockout cells. Heterochromatin
323 protein (HP)1α is a central component of heterochromatin in mammalian and *Drosophila* cells
324 (Saksouk et al. 2015). The number of HP1α-labeled spot areas increased in β-actin knockout
325 cells (Xie et al. 2018). This increase in the heterochromatin area in β-actin knockout cells is
326 similar to the increased chromocenter size in *act7*. In mammalian cells, β-actin is an essential
327 component of the chromatin remodeling complex BRG1/BRM-associated factor (BAF,
328 mammalian SWI/SNF) (Kapoor and Shen 2014). β-actin is required for maximum ATPase
329 activity of Brg1, an ATPase subunit of the BAF complex. Loss of β-actin significantly decreased
330 DNA binding of Brg1 (Xie et al. 2018). Therefore, β-actin regulates heterochromatin
331 organization through its DNA-binding activity of the BAF complex (Xie et al. 2018). In plants,
332 orthologs of SWI/SNF subunits have been identified, and their functions have been characterized
333 (Reyes 2014, Nishioka et al. 2020). The interaction between actin and BRM has not yet been
334 reported in plants, but our results suggest that plant actin also plays a role in regulating the
335 activities of the chromatin remodeling complex, which regulates heterochromatin organization
336 and gene expression. In this scenario, loss of ADF stabilizes AFs, decreases the available actin
337 monomers, thus affecting actin-mediating regulation of chromatin organization and gene
338 expression.
339 Another possibility is that ADF and ACT regulate chromatin organization through
340 regulation of cytoplasmic AFs, which are connected with chromatin through the nuclear
341 envelope-embedded protein complex and nuclear lamina. Mammalian genomes have three
342 ADFs, namely, Cofilin-1 (COF), ADF, and COF-2. The depletion of both COF and ADF
343 expression induces severe deformation of nuclear shape in mice (Kanellos et al. 2015) and in
344 several mammalian cultured cells, including HeLa cells (Wiggan et al. 2017). COF/ADF-
345 depleted HeLa cells exhibit a significant reduction in the level of H3K27me3, which marks
346 facultative heterochromatin at the nuclear periphery (Wiggan et al. 2017). The nuclear

347 deformation in COF/ADF-silenced cells is associated with excessive activation of myosin-II in
348 the cytoplasm and disruption of the nuclear lamina (Wiggan et al. 2017). The cytoplasmic AFs
349 are connected with the nuclear envelope-embedded linker of the nucleoskeleton and cytoskeleton
350 complex, which is composed of outer nuclear envelope-localized Klarsicht, ANC-1, and SYNE
351 homology (KASH) domain-containing nesprins and inner nuclear envelope-localized SUN (Sad1
352 and UNC-84) domain-containing proteins (Tamura et al. 2015). SUN proteins interact with
353 nuclear lamina (Tamura et al. 2015), and nuclear lamina interact with heterochromatin (Hoskins
354 et al. 2021). Nuclei in COF/ADF-depleted mammalian cells show the disorganization of the
355 nuclear lamina, and the authors concluded that excessive tension in the cytoplasm caused by the
356 depletion of COF/ADF results in alterations in nuclear organization and gene expression
357 (Wiggan et al. 2017).
358 The reduction of H3K27me3 level in COF/ADF-depleted HeLa cells resembles the
359 reduction in the size of chromocenters in *adf4* and *ADF1-4Ri*. Our results that chromocenters at
360 the nuclear periphery were more strongly affected compared with those near the nucleoli in *adf4*,
361 *ADF1-4Ri* and *act7* (see Figs. 1H, 1I and 3H) also support this hypothesis that connection
362 between cytoplasmic AFs and chromatin through nuclear envelope-embedded protein complex is
363 important for regulation of chromatin organization. Indeed, the clustered chromocenters in
364 *ADF1-4Ri* (Fig. S4) were similar to the polarized organization of chromocenters observed in *A.*
365 *thaliana* mutants of KASH and SUN (Sakamoto et al. 2022). Our result of *fiz1* (Fig. S5),
366 however, does not support this hypothesis. While cytoplasmic AFs are highly disrupted (Kato et
367 al. 2010), *fiz1* did not show alteration in chromocenter size.
368 The result of *fiz1* supports the third hypothesis, in which the function of ADF in the
369 nucleus, rather than in the cytoplasm, could contribute to the regulation of chromocenter
370 organization. In mammalian cells, it has been shown that nuclear AFs are transiently formed
371 upon various stimuli and regulate gene expression, DNA damage repair, and regulation of
372 nuclear size (Percipalle and Vartiainen 2019). Subclass I ADFs and ACT may regulate
373 heterochromatin organization and gene expression through a regulation of nuclear AFs, which
374 has not been reported in plant cells yet. It is also possible that ADF and ACT function in a
375 separate pathway to regulate chromatin organization and gene expression.
376 We showed that genes related to plant defense response are both up- and downregulated in
377 *adf4* and *ADF1-4Ri*. Furthermore, we found that expression of many *NLR* genes are
378 downregulated in *adf4* and *ADF1-4Ri*. Twenty-two *NLRs* showed reduced expression in both
379 *adf4* and *ADF1-4Ri*. While our microarray analysis used uninfected mature leaves, it has been
380 shown that *RPS5* expression, of which reduction was confirmed in our microarray, was reduced
381 both in uninfected and *Pst* AvrPphB-infected *adf4* (Porter et al. 2012), suggesting that *NLR*
382 expression is also affected in *adf4* and *ADF1-4Ri* during pathogen infection. Our result that
383 expression of some *NLRs* was suppressed only in *adf4* or in *ADF1-4Ri* suggests that different
384 ADF members affect expression of different sets of *NLR*s. This could explain previous results
385 where loss of *ADF*s results in both increase or decrease in resistance depending on pathogens
386 and that different ADF members affect pathogen response differently. Tian et al. reported that *A.*

387 *thaliana adf4* showed an increased susceptibility against the bacterial pathogen *Pst* harboring
388 AvrPphB, whereas *adf4* showed comparable susceptibility against *Pst* or *Pst* AvrB. Neither *adf1*
389 nor *adf3* showed altered susceptibility against these pathogens. The susceptibility of *ADF1-4Ri*
390 against *Pst* AvrPphB was also comparable with that of Col-0 (Tian et al. 2009). However, both
391 *adf4* and *ADF1-4Ri* showed an increased resistance to *G. orontii* (Inada et al. 2016). In wheat
392 (*Triticum aestivum* L.), the suppression of different members of ADFs has different effects on
393 immunity against fungus causing stripe rust. Wheat genotype Suwon 11 is resistance to *Puccinia*
394 *striiformis* f.sp. *tritici* CYR23 but is susceptible to *P. striiformis* f.sp. *tritici* CYR31. Knockdown
395 of *TaADF7* (Fu et al. 2014) and *TaADF4* (Zhang et al. 2017) both increased a susceptibility
396 against CYR23. By contrast, knockdown of *TaADF3* expression caused increased resistance
397 against CYR31 (Tang et al. 2016). It is possible that TaADF3, 4, and 7 affect the expression of
398 different set of *NLR*s, which results in the above-mentioned phenotypic differences.
399 Taken together, our results strongly suggests that *A. thaliana* subclass I ADFs regulate
400 various aspects of plant physiology including pathogen response through their roles in regulation
401 of nuclear organization and gene expression. Future research elucidating the mechanism how
402 ADFs and actin regulate nuclear organization and gene expression will contribute to understand
403 the new roles of plant cytoskeletons as well as new mechanisms regulating gene expression.
404
405
406 **MATERIALS AND METHODS**
407
408 **Plant materials and growth condition**
409 *adf4* (Garlic_823_A11b.1b.Lb3Fa) and *ADF1-4Ri* lines were described previously (Tian et al.
410 2009). The loss of *ADF4* transcript in *adf4* was previously examined (Tian et al. 2009). *act2-*
411 *1/act8-2* double mutant and *act7-4* single mutant were described previously (Kandasamy et al.
412 2009). *act2-1* and *act7-4* were identified in mutant screenings of T-DNA insertion lines
413 ((McKinney et al. 1995, Gilliland et al. 2003). *ACT2* transcript in *act2-1* is severely knocked
414 down with <4% of wild type, while both *act7-4* and *act8-2* (GABi-Kat line 480C07) show low
415 level of *ACT7* and *ACT8* transcripts, respectively, at 10~15% of wild type (Kandasamy et al.
416 2009). *Arabidopsis* seeds were suspended in autoclaved 0.1% agarose and incubated at 4°C for
417 vernalization for more than 1 day (up to 2 weeks) before direct sowing on 1:3
418 metromix:vermiculite in plastic pots. Entire pots were covered with plastic wrap for 1 week after
419 sowing to maintain humidity and to encourage germination. Plants were grown at 22°C in a
420 growth chamber under a 16-h light:8-h dark photoperiod (LH-411S, NK Systems, Osaka, Japan).
421
422 **Observation of chromocenters**
423 For observation of chromocenters in epidermal cells, 4 week old mature leaves were fixed with
424 3:1 ethanol:acetic acid at R.T. overnight. Fixed leaves were then rinsed with milliQ three times
425 before stained with 1 μg/mL DAPI. Images of DAPI-stained nuclei in epidermal cells were
426 excited with 405 nm laser, and fluorescence between 410-585 nm was captured using confocal
427 laser scanning microscope (Zeiss LSM700) that was equipped with ×63 objective lens (N.A.
428 1.4). Z-stack images were obtained with 0.5 μm step size.

429
430 **Quantitative image analysis of chromocenters**
431 Obtained Z-stack confocal images of DAPI were combined using maximum intensity projection.
432 To measure the chromocenter number and size, a binary image was obtained from the maximum
433 intensity projection image by intensity thresholding. Before binarization, a Gaussian filter (sigma
434 = 2 pixels) was applied to the images in order to improve the signal to noise ratio. Intensity
435 thresholding was performed based on Yen's method (Yen et al. 1995), and then the binary
436 images were masked by manually segmented nuclear regions. Number and size of the
437 chromocenter blobs in the binary images were measured. All image processing and analysis were
438 performed by ImageJ software (Schneider et al. 2012).
439
440 **Microarray analysis**
441 4-week old mature leaves were harvested and frozen in liquid N_2. Total RNA was extracted
442 using TRIzol reagent (Life Technologies Japan, Tokyo, Japan) and purified with an RNeasy
443 Micro kit (Qiagen) following the manufacturers' instructions. Arabidopsis Gene 1.0 ST arrays
444 (Thermo Fisher Scientific) was used for microarray analysis. Quality of RNA was checked using
445 RNA 600 Nano LabChip Kit (Agilent) following the manufacturer's protocol. Sense-strand DNA
446 target preparation was performed with WT Expression Kit (Ambion) and GeneChip WT
447 Terminal labeling Kit and Controls Kit (Thermo Fisher Scientific) following the manufacturer's
448 protocols. Hybridization, washing, and staining procedures were performed on Fluidics Station
449 450 (Affymetrix) with GeneChip Hybridization, Wash, and Stain Kit (Thermo Fisher Scientific).
450 GeneChips were scanned with GeneChip Scanner 3000 7G. Gene-level RMA sketch
451 normalization was performed using standard settings for GeneChip Gene 1.0 ST arrays on
452 Expression Console Version 1.3 (Affymetrix). Microarray data were quantified using
453 Transcriptome Analysis Console 4.0 (Thermo Fisher Scientific). Expression levels were
454 compared between Col-0 and *adf4* and between Col-0 and *ADF1-4Ri* by calculating average log2
455 ratios. Genes with significantly altered expression were defined as those with a fold change of ≥2
456 or ≤-2 from Col-0 for both *adf4* and *ADF1-4Ri*. GO analysis was performed using PANTHER
457 17.0 (Released 20220223). Microarray data were deposited in Gene Expression Omnibus (GEO)
458 of National Center for Biotechnology Information (NCBI) and are accessible through GEO
459 accession number GSE228396.
460
461 **qRT-PCR**
462 Mature leaves were harvested from 4-week-old plants and frozen in liquid N_2. Total RNA was
463 extracted using TRIzol reagent (Life Technologies Japan, Tokyo, Japan) in accordance with the
464 manufacturer's protocol. cDNA was synthesized with the ReverTra Ace qPCR RT Master Mix
465 with gDNA Remover (TOYOBO) using 100 ng of total RNA. qRT-PCR was carried out using
466 THUNDERBIRD SYBR qPCR Mix (TOYOBO) on 7300 Real Time PCR System (Applied
467 Biosystems). *ACT8* (At1g49240) was used as internal control gene for normalization. Primer
468 information is shown in Table S5.

469
470
471 **DATA AVAILABILITY**
472 The microarray data used in this article are available in NCBI GEO (National Center for
473 Biotechnology Information Gene Expression Omnibus) and can be accessed with GSE228396.
474
475 **FUNDING INFORMATION**
476 This work was supported by Grants-in-Aid for Scientific Research (21H04715 for MU,
477 16K07415 and 20K06690 for NI), the Osaka Prefecture University internal fund "RESPECT",
478 Osumi Frontier Science Foundation, the NOVARTIS Foundation (Japan) for the Promotion of
479 Science, and Yamada Science Foundation for NI.
480
481 **ACKNOWLEDGEMENT**
482 We thank Prof. Brad Day for his generous gift of *ADF1-4Ri* lines. We also thank Prof. Richard
483 B. Meagher for his gift of *act2/8* and *act7*, Prof. Masao Tasaka and Dr. Takehide Kato for
484 generous gift of *fiz1*, and Prof. Kyoko Itoh and Ms. Yukiko Sugisawa in University of Tokyo for
485 their help in performing microarray analysis.
486
487
488 **REFERENCES**
489
490 An, Y-Q., McDowell, J.M., Huang, S., McKinney, E.C., Chambliss, S., and Meagher, R.B.
491 (1996) Strong, constitutive expression of the *Arabidopsis ACT2/ACT8* actin subclass in
492 vegetative tissues. Plant J. 10, 107-121.
493 Axelsen, K.B., and Palmgren, M.G. (2001) Inventory of the superfamily of P-type ion pumps in
494 Arabidopsis. Plant Physiol. 126, 696-706.
495 Baarlink, C., Wang, H., and Grosse, R. (2013) Nuclear actin network assembly by formins
496 regulates the SRF coactivator MAL. Science 340, 864-867.
497 Burgos-Rivera, B., Ruzicka, D.R., Deal, R.B., McKinney, E.C., King-Reid, L., and Meagher,
498 R.B. (2008) *ACTIN DEPOLYMERIZING FACTOR9* controls development and gene expression
499 in *Arabidopsis*. Plant Mol Biol. 68, 619-632.
500 Cartagena, J.A., Matsunaga, S., Seki, M., Kurihara, D., Yokoyama, M., Shinozaki, K. et al.
501 (2008) The *Arabidopsis* SDG4 contributes to the regulation of pollen tube growth by methylation
502 of histone H3 lysines 4 and 36 in mature pollen. Dev. Biol. 315, 355-368.
503 Chen, K., Fan, B., Du, L., and Chen, Z. (2004) Activation of hypersensitive cell death by
504 pathogen-induced receptor-like protein kinases from *Arabidopsis*. Plant Mol. Biol. 56, 271-283.
505 Clément, M., Ketelaar, T., Rodiuc, N., Banora, M.Y., Smertenko, A., Engler, G., et al. (2009)
506 Actin-Depolymerizing Factor2-mediated actin dynamics are essential for root-knot nematode
507 infection of *Arabidopsis*. Plant Cell 21, 2963-2979.

508 Davidson, P.M., and Cadot, B. (2021) Actin on and around the nucleus. Trend. Cell Biol. 31,
509 211-223.
510 Devoto, A., Ellis, C., Magusin, A., Chang, H-S., Chilcott, C., Zhu, T., et al. (2005) Expression
511 profiling revelas COI1 to be a key regulator of genes involved in wound- and methyl jasmonate-
512 induced secondary metabolism, defence, and hormone interactions. Plant Mol. Biol. 58, 497-513.
513 Dong, C-H., Xia, G-X., Hong, Y., Ramachandran, S., Kost, B., and Chua, N-H. (2001) ADF
514 proteins are involved in the control of flowering and regulate F-actin organization, cell expansion
515 and organ growth in Arabidopsis. Plant Cell 13, 1333-1346.
516 Dubos, C., Stracke, R., Grotewold, E., Weisshaar, B., Martin C., and Lepniec, L. (2010) MYB
517 transcription factors in *Arabidopsis*. Trend. Plant Sci. 15, 573-581.
518 Eggermont, L., Verstraeten, B., and Van Damme E.J.M. (2017) Genome-wide screening for
519 lectin motifs in *Arabidopsis thaliana*. Plant Genome 10. Doi: 10.3835/plantgenome2017.02.0010
520 Fick, A., Swart, V., and van den Berg, N. (2022) The ups and downs of plant NLR expression
521 during pathogen infection. Front. Plant Sci. 13, 921148.
522 Fransz, P., de Jong, J.H., Lysak, M., Castiglione, M.R., and Schubert, I. (2002) Interphase
523 chromosomes in *Arabidopsis* are organized as well defined chromocenters from which
524 euchromatin loops emanate. Proc. Natl. Acad. Sci., U.S.A. 99, 14584-14589.
525 Fu, Y., Duan, X., Tang, C., Li, X., Voegele, R.T., Wang, X. et al. (2014) TaADF7, an actin-
526 depolymerizing factor, contributes to wheat resistance against *Puccinia striiformis* f.sp. *tritici*.
527 Plant J. 78, 16-30.
528 Gilliland, L.U., Pawloski, L.C., Kandasamy, M.K., and Meagher, R.B. (2003) *Arabidopsis* actin
529 gene ACT7 plays an essential role in germination and root growth. Plant J. 33, 319-328.
530 Han, Y., Watanabe, S., Shimada, H., and Sakamoto, A. (2020) Dynamics of the leaf endoplasmic
531 reticulum modulate β-glucosidase-mediated stress activated ABA production from its glucosyl
532 ester. J. Exp. Bot. 71, 2058-2071.
533 Henty, J.L., Bledsoe, S.W., Khurana, P., Meagher, R.B., Day, B., Blanchoin, L., et al. (2011)
534 Arabidopsis Actin Depolymerizing Factor 4 modulates the stochastic dynamic behavior of actin
535 filaments in the cortical array of epidermal cells. Plant Cell 23, 3711-3726.
536 Henty-Ridilla, J.L., Li, J., Blanchoin, L., and Staiger, C.J. (2013) Actin dynamics in the cortical
537 array of plant cells. Curr. Opin. Plant Biol. 16, 678-687.
538 Hoskins, V.E., Smith, K., and Reddy, K.L. (2021) The shifting shape of genomes: dynamics of
539 heterochromatin interactions at the nuclear lamina. Curr. Opin. Gene. Dev. 67, 163-173.
540 Hurst, V., Shimada, K., and Gasser, S.M. (2019) Nuclear actin and actin-binding proteins in
541 DNA repair. Trend. Cell Biol. 29, 462-476.
542 Imaizumi, C., Tomatsu, H., Kitazawa, K., Yoshimi, Y., Shibano, S., Kikuchi, K. et al. (2017)
543 Heterologous expression and characterization of an Arabidopsis β-$_L$-arabinopyranosidase and α-
544 $_D$-galactosidases acting on β-$_L$-arabinopyranosyl residues. J. Exp. Bot. 68, 4651-4661.
545 Inada, N., Higaki, T., and Hasezawa, S. (2016) Nuclear function of subclass I Actin
546 Depolymerizing Factor contributes to susceptibility in Arabidopsis to an adapted powdery
547 mildew fungus. Plant Physiol. 170, 1420-1434.

548 Inada, N. (2017) Plant Actin Depolymerizing Factor – Actin microfilament disassembly and
549 more. J. Plant Res. 130, 227-238.
550 Inada, N., Takahashi, N., and Umeda, M. (2021) Arabidopsis thaliana subclass I ACTIN
551 DEPOLYMERIZING FACTORs and vegetative ACTIN2/8 are novel regulators of
552 endoreplication. J. Plant Res. 134, 1291-1300.
553 Jansson, S. (1999) A guide to the Lhc genes and their relatives in Arabidopsis. Trend. Plant Sci.
554 4, 236-240.
555 Kandasamy, M.K., McKinney, E.C., and Meagher, R.B. (2009) A single vegetative actin
556 isovariant overexpressed under the control of multiple regulatory sequences in sufficient for
557 normal Arabidopsis development. Plant Cell 21, 701-718.
558 Kandasamy, M.K., McKinney, E.C., and Meagher, R.B. (2010) Differential sublocalization of
559 actin variants within the nucleus. Cytoskeleton 67, 729-743.
560 Kanellos, G., Zhou, J., Patel, H., Ridgway, R.A., Huels, D., Gurniak, C.B. et al. (2015) ADF and
561 Cofilin1 control actin stress fibers, nuclear integrity, and cell survival. Cell Rep. 13, 1949-1964.
562 Kapoor, P., and Shen, X. (2014) Mechanisms of nuclear actin in chromatin remodeling
563 complexes. Trend. Cell Biol. 24, 238-246.
564 Kato, T., Terao Morita, M., and Tasaka, M. (2010) Defects in dynamics and functions of actin
565 filament in Arabidopsis caused by the dominant-negative actin *fiz1*-induced fragmentation of
566 actin filament. Plant Cell Physiol. 51, 333-338.
567 Lu, K., Liang, S., Wu, Z., Bi, C., Yu, Y-T., Wang, X-F. et al. (2016) Overexpression of an
568 Arabidopsis cysteine-rich receptor-like protein kinase, CRK5, enhances abscisic acid sensitivity
569 and confers drought tolerance. J. Exp. Bot. 67, 5009-5027.
570 McDowell, J.M., Huang, S., McKinney, E.C., An, Y-Q., and Meagher, R.B. (1996a) Structure
571 and evolution of the actin gene family in *Arabidopsis thaliana*. Genetics 142, 587-602.
572 McDowell, J.M., An, Y-Q., Huang, S., McKinney, E.C., and Meagher, R.B. (1996b) The
573 Arabidopsis *ACT7* actin gene is expressed in rapidly developing tissues and responds to several
574 external stimuli. Plant Physiol. 111, 699-711.
575 McDowell, J.M., Cuzick, A., Can, C., Beynon, J., Dangl, J.L., and Holub, E.B. (2000) Downy
576 mildew (*Peronospora parasitica*) resistance genes in Arabidopsis vary in functional
577 requirements for *NDR1*, *EDS1*, *NPR1* and salicylic acid accumulation. Plant J. 22, 523-529.
578 McKinney, E.C., Ali, N., Traut, A., Feldmann, K.A., Belostotsky, D.A., McDowell, J.M. et al.
579 (1995) Sequence-based identification of T-DNA insertion mutations in *Arabidopsis*: actin
580 mutants *act2-1* and *act4-1*. Plant J. 8, 613-622.
581 McKinney, E.C., and Meagher, R.C. (1998) Members of the Arabidopsis actin gene family are
582 widely dispersed in the genome. Genetics 149, 663-675.
583 Mlynárová, L., Nap, L-P., and Besseling, T. (2007) The SWI/SNF chromatin-remodeling gene
584 *AtCHR12* mediates temporary growth arrest in Arabidopsis thaliana upon perceiving
585 environmental stress. Plant J. 51, 874-885.

586 Mondal, H.A., Louis, J., Archer, L., Patel, M., Nalam, V.J., Sivapalan, V., et al. (2018)
587 Arabidopsis *ACTIN-DEPOLYMERIZING FACTOR3* is required for controlling aphid feeding
588 from the phloem. Plant Physiol.176, 879-890.
589 Nishioka, S., Sakamoto, T., and Matsunaga, S. (2020) Role of BRAHMA and its interacting
590 partners in plant chromatin remodeling. Cytologia 85, 263-267.
591 Ogasawara, K., Yamada, K., Christeller, J.T., Kondo, M., Hatsugai, N., Hara-Nishimura, I. et al.
592 (2009) Constitutive and inducible ER bodies of *Arabidopsis thaliana* accumulate distinct β -
593 glucosidases. Plant Cell Physiol. 50, 480-488.
594 Ortega-Ortega, Y., Carrasco-Castilla, J., Juárez-Verdayes, M.A., Toscano-Morales, R., Fonseca-
595 García, C., Nava, N., et al. (2020) Actin Depolymerizing Factor modulates rhizobial infection
596 and nodule organogenesis in common bean. Int. J. Mol. Sci. 21, 1970.
597 Percipalle, P., and Vartiainen, M. (2019) Cytoskeletal proteins in the cell nucleus: a special
598 nuclear actin perspective. Mol. Biol. Cell 30, 1781-1785.
599 Pietrzykowska, M., Suorsa, M., Semchonok, D.A., Tikkanen, M., Boekema, E.J., Aro, E-M., et
600 al. (2014) The light-harvesting chrolophyll *a/b* binding proteins Lhcb1 and Lhcb2 play
601 complementary roles during state transitions in *Arabidopsis*. Plant Cell 26, 3646-3660.
602 Pok Man Ngou, B., Ding, P., and Jones, J.D.G. (2022) Thirty years of resistance : Zig-zag
603 through the plant immune system. Plant Cell 34, 1447-1478.
604 Porter, K., and Day, B. (2013) Actin branches out to link pathogen preception and host gene
605 regulation. Plant Sign. Behav. 8, e23468.
606 Porter, K., and Day, B. (2016) From filaments to function: the role of the plant actin cytoskeleton
607 in pathogen perception, signaling and immunity. J. Intergr. Plant Biol. 58, 299-311.
608 Porter, K., Shimono, M., Tian, M., and Day, B. (2012) Arabidopsis Actin-Depolymerizing
609 Factor-4 links pathogen perception, defense activation and transcription to cytoskeletal
610 dynamics. PLOS Pathogens 8, e1003006.
611 Qian, D., Zhang, Z., He, J., Zhang, P., Ou, X., Li, T., et al. (2019) Arabidopsis ADF5 promotes
612 stomatal closure by regulating actin cytoskeleton remodeling in response to ABA and drought
613 stress. J. Exp. Bot. 70, 435-446.
614 Reyes, J.C. (2014) The many faces of plant SWI/SNF complex. Mol. Plant 7, 454-458.
615 Ruzicka, D.R., Kandasamy, M.K., McKinney, E.C., Burgos-Rivera, B., and Meagher, R.B.
616 (2007) The ancient subclasses of Arabidopsis ACTIN DEPOLYMERIZING FACTOR genes
617 exhibit novel and differential expression. Plant J. 52, 460-472.
618 Sakamoto, T., Sakamoto, Y., Grob, S., Slane, D., Yamashita, T., Ito, N. et al. (2022) Two-step
619 regulation of centromere distribution by condensin II and the nuclear envelope proteins. Nat.
620 Plants 8, 940-953.
621 Saksouk, N., Simboeck, E., and Déjardin, J. (2015) Constitutive heterochromatin formation and
622 transcription in mammals. Epigene. Chrom. 8, 3.
623 Sasaki-Sekimoto, Y., Taki, N., Obayashi, T., Aono, M., Matsumoto, F., Sakurai, N. et al. (2005)
624 Coodinated activation of metabolic pathways for antioxidants and defence compounds by
625 jasmonates and their roles in stress tolerance in Arabidopsis. Plant J. 44, 653-668.

626 Schneider, C.A., Rasband, W.S., and Eliceiri, K.W. (2012) NIH Image to ImageJ: 25 years of
627 image analysis. Nat. Methods 9, 671–675. doi:10.1038/nmeth.2089
628 Sengupta, S., Mangu, V., Sanchez, L., Bedre, R., Joshi, R., Rajasekaran, K., et al. (2019) An
629 actin-depolymerizing factor from the halophyte smooth cordgrass, *Spartina alterniflora*
630 (SaADF2), is superior to its rice homolog (OsADF2) in conferring drought and salt tolerance
631 when constitutively overexpressed in rice. Plant Biotech. J. 17, 188-205.
632 Sun, Y., Zhong, M., Li, Y., Zhang, R., Su, L., Xia, G., et al. (2021) *GhADF6*-mediated actin
633 reorganization is associated with defence against *Verticillium dahliae* infection in cotton. Mol.
634 Plant Pathol. 22, 1656-1667.
635 Sweat, T.A., and Wolpert, T.J. (2007) Thioredoxin *h5* is required for victorin sensitivity
636 mediated by a CC-NBS-LRR gene in *Arabidopsis*. Plant Cell 19, 673-687.
637 Takemoto, D., Jones, D.A., and Hardham, A.R. (2003) GFP-tagging of cell components reveals
638 the dynamics of subcellular re-organization in response to infection of *Arabidopsis* by oomycete
639 pathogens. Plant J. 33, 775-792.
640 Tamura, K., Goto, C., and Hara-Nishimura, I. (2015) Recent advances in understanding plant
641 nuclear envelope proteins involved in nuclear morphology. J. Exp. Bot. 66, 1641-1647.
642 Tang, C., Deng, L., Chen, S., Wang, X., and Kang, Z. (2016) TaADF3, an Actin-Depolymerizing
643 Factor, negatively modulates wheat resistance against *Puccinia striiformis.* Front. Plant Sci. 6,
644 1214.
645 Tian, M., Chaudhry, F., Ruzicka, D.R., Meagher, R.B., Staiger, C.J., and Day, B. (2009)
646 Arabidopsis Actin-Depolymerizing Factor AtADF4 mediates defense signal transduction
647 triggered by the *Pseudomonas syringae* effector AvrPphB. Plant Physiol. 150, 815-824.
648 Xie, X., Almuzzaini, B., Drou, N., Kremb, S., Yousif, A., Farrants, A-K.Ö., et al. (2018) β-
649 Actin-dependent global chromatin organization and gene expression programs control cellular
650 identity. FASEB J. 32, 1296-1314.
651 Xu, K., Zhao, Y., Zhao, S., Liu, H., Wang, W., Zhang, S., et al. (2021) Genome-wide
652 identification and low temperature responsive pattern of actin depolymerizing factor (ADF) gene
653 family in wheat (*Triticum aestivum* L.). Front. Plant Sci. 12, 618984.
654 Yeh, Y-H., Chang, Y-H., Huang, P-Y., Huang, J-B., and Zimmerli, L. (2015) Enhanced
655 Arabidopsis pattern-triggered immunity by overexpression of cysteine-rich receptor-like kinases.
656 Front. Plant Sci. 6, 322.
657 Yen, J.C., Chang, F.J., and Chang, S. (1995) A new criterion for automatic multilevel
658 thresholding. IEEE Trans. on Image Processing 4, 370-378.
659 Wang, L., Qiu, T., Yue, J., Guo, N., He, Y., Han, Y., et al. (2021) *Arabidopsis ADF1* is regulated
660 by MYB73 and is involved in response to salt stress affecting actin filament organization. Plant
661 Cell Physiol. 62, 1387-1395.
662 Wiggan, O., Chroder, B., Krapf, D., Bamburg, J.R., and DeLuca, J.G. (2017) Cofilin regulates
663 nuclear architecture through a myosin-II dependent mechanotransduction module. Sci. Rep. 7,
664 40953.

665 Zhang, B., Hua, Y., Wang, J., Huo, Y., Shimono, M., Day, M., et al. (2017) *TaADF4*, an actin-
666 depolymerizing factor from wheat, is required for resistance to the stripe rust pathogen *Puccinia*
667 *striiformis* f. sp. *tritici*. Plant J. 89, 1210-1224.
668 Zhu, Q-H., Stephen, S., Kazan, K., Jin, G., Fan, L., Taylor, J. et al. (2013) Characterization of
669 the defense transcriptome responsive to *Fusarium oxysporum*-infection in *Arabidopsis* using
670 RNA-seq. Gene 512, 259-266.
671
672
673

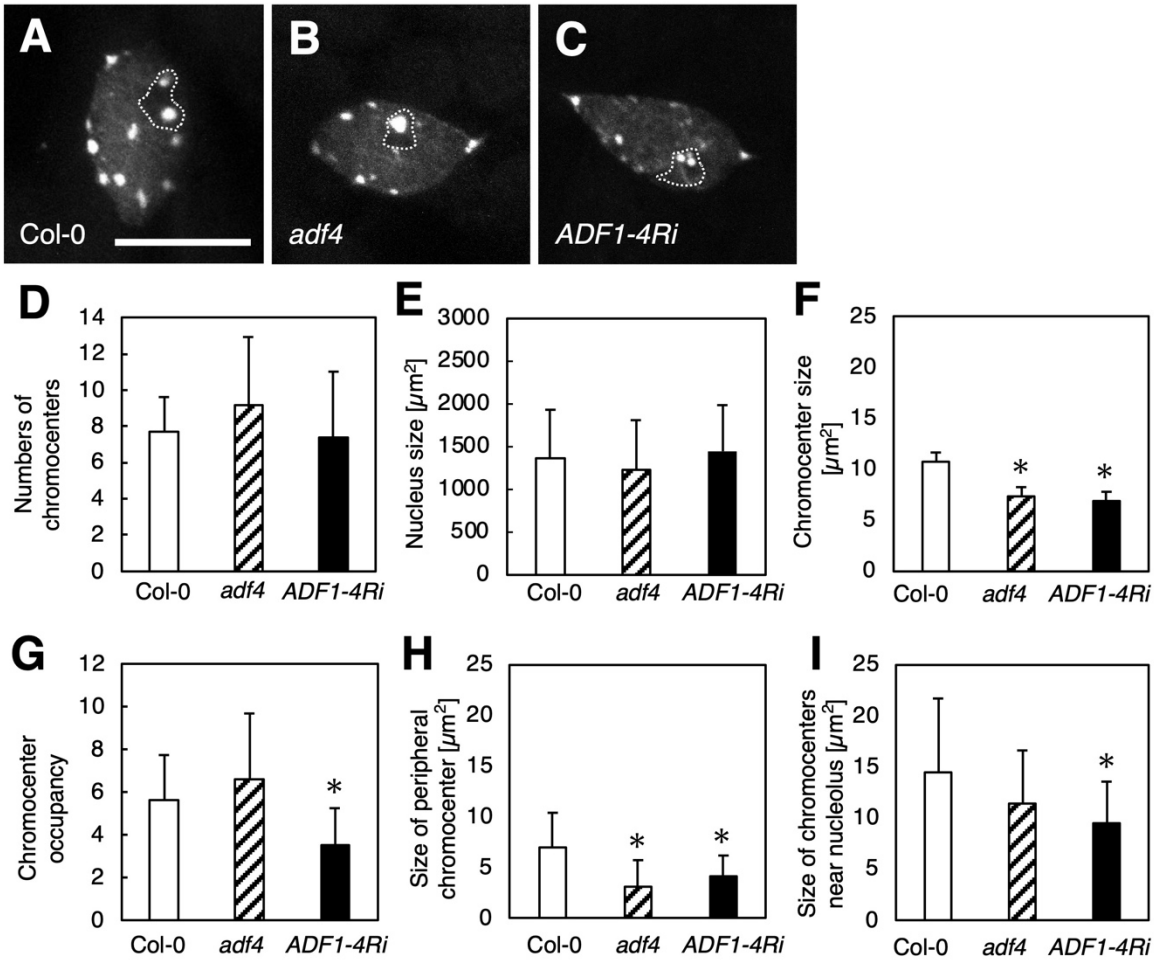

Figure 1. The size of chromocenters was reduced in *adf4* and *ADF1-4Ri* mature leaves. The fluorescence micrographs of DAPI-stained nuclei in epidermal cells of mature leaves in Col-0 (**A**), *adf4* (**B**), and *ADF1-4Ri* (**C**). Dotted lines indicate nucleoli. Bar indicates 5 µm. (**D**) Numbers of chromocenters, (**E**) the size of nuclei, (**F**) the size of chromocenters, (**G**) the percentage of chromocenter area in nuclei, (**H**) the size of chromocenters located at the nuclear periphery, and (**I**) the size of chromocenters located near the nucleoli in Col-0, *adf4*, and *ADF1-4Ri* were quantified using fluorescence micrographs. Twentyfour -27 nuclear images were used for quantitative analysis. Comparison with Col-0 was performed by Student's *t*-test. Asterisks indicate that there is a significant difference (* $P<0.05$).

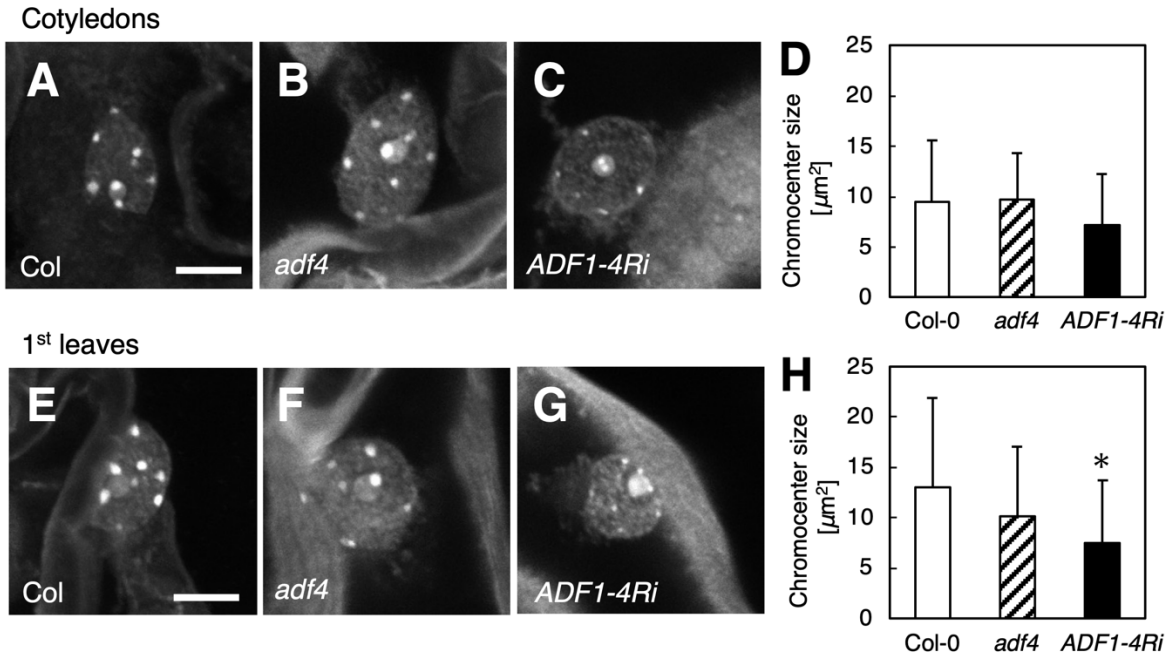

Figure 2. The size of chromocenters was less affected in cotyledons of *adf4* and *ADF1-4Ri*. The fluorescence micrographs of DAPI-stained nuclei in epidermal cells of cotyledons in Col-0 (**A**), *adf4* (**B**), and *ADF1-4Ri* (**C**). (**D**) The size of chromocenters in Col-0, *adf4*, and *ADF1-4Ri* cotyledons. Twelve nuclear images each were used to obtain average size of chromocenters. The fluorescence micrographs of DAPI-stained nuclei in epidermal cells of 1st leaves in Col-0 (**E**), *adf4* (**F**), and *ADF1-4Ri* (**G**). (**H**) The size of chromocenters in Col-0, *adf4*, and *ADF1-4Ri* 1st leaves. Twelve nuclear images each were used to obtain average size of chromocenters. Bars indicate 5 μm. Comparison with Col-0 was performed by Student's *t*-test. Asterisks indicate that there is a significant difference (* $P<0.05$).

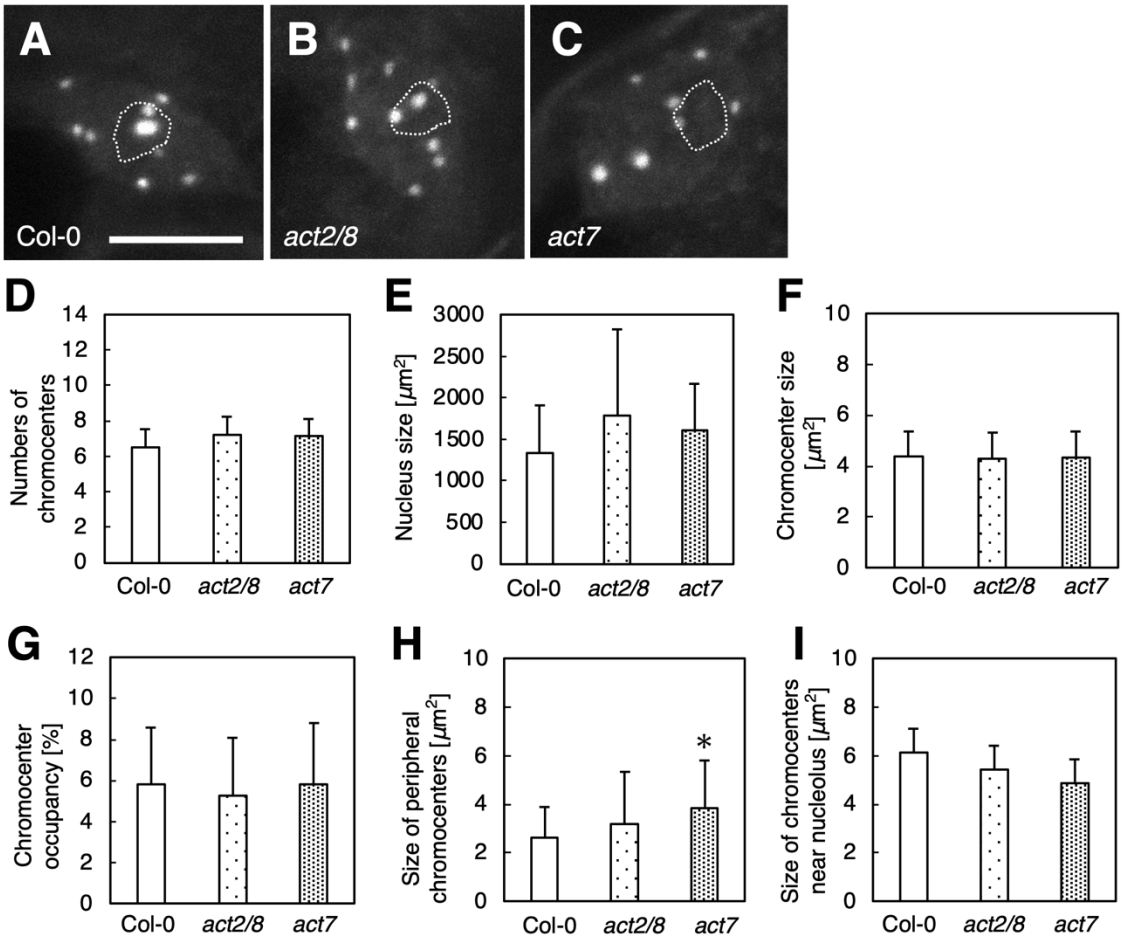

Figure 3. The size of chromocenters was increased in *act7* mature leaves. The fluorescence micrographs of DAPI-stained nuclei in epidermal cells of mature leaves in Col-0 (**A**), *act2/8* (**B**), and *act7* (**C**). Dotted lines indicate nucleoli. Bar indicates 5 µm. (**D**) Numbers of chromocenters, (**E**) the size of nuclei, (**F**) the size of chromocenters, (**G**) the percentage of chromocenter area in nuclei, (**H**) the size of chromocenters located at the nuclear periphery, and (**I**) the size of chromocenters located near the nucleoli in Col-0, *act2/8*, and *act7* were quantified using fluorescence micrographs. Sixteen – 19 nuclear images were used for quantitative analysis. Comparison with Col-0 was performed by Student's *t*-test. Asterisks indicate that there is a significant difference (* $P<0.05$).

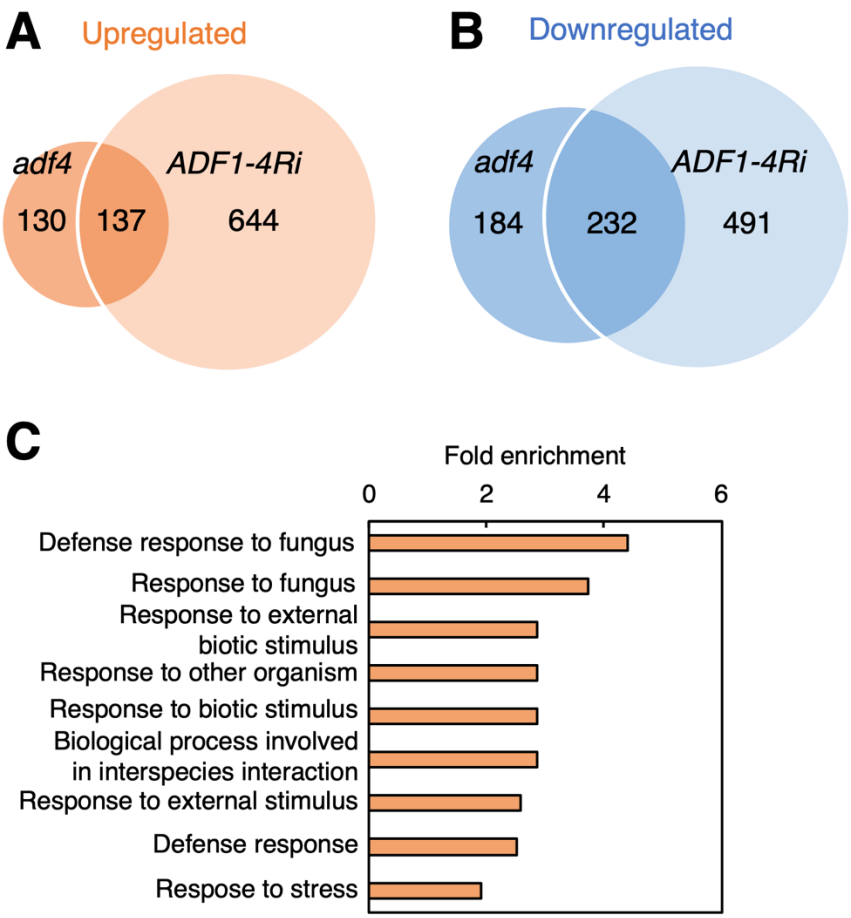

713
714
715 **Figure 4.** Microarray analysis showed altered expression of many genes in *adf4* and *ADF1-4Ri*
716 mature leaves. Venn diagrams of upregulated (**A**) and downregulated (**B**) genes in *adf4* and
717 *ADF1-4Ri*. (**C**) GO analysis for genes that showed altered expression in both *adf4* and *ADF1-4Ri*
718 (genes including both upregulated and downregulated genes).
719
720

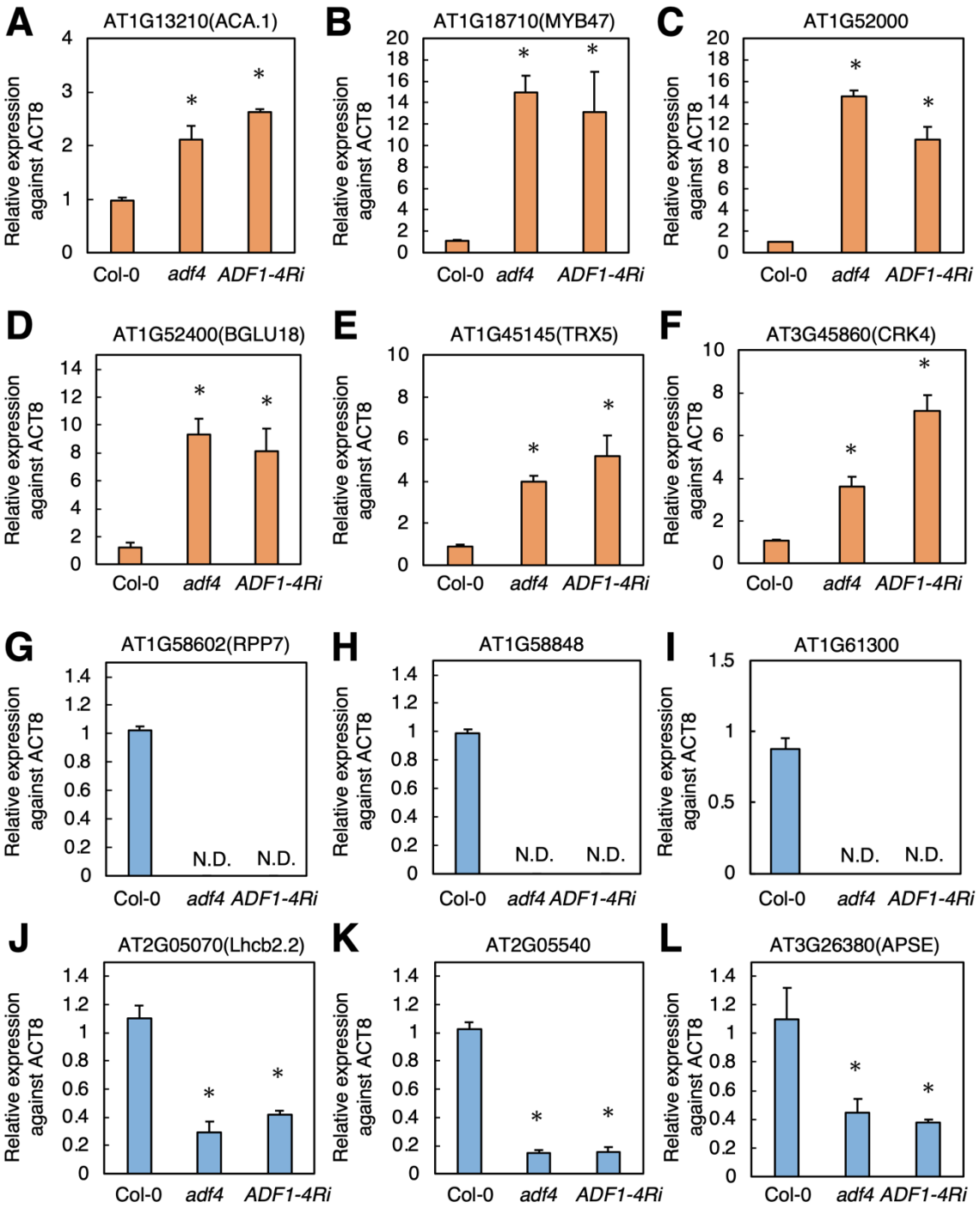

Figure 5. qRT-PCR confirmed alteration in gene expression in *adf4* and *ADF1-4Ri* shown by microarray analysis. The expression of At1g13210 (**A**), At1g18710 (**B**), At1g52000 (**C**), At1g52400 (**D**), At1g45145 (**E**), and At3g45860 (**F**) was upregulated in both *adf4* and *ADF1-4Ri*. The expression of At1g58602 (**G**), At1g58848 (**H**), At1g61300 (**I**), At2g05070 (**J**), At2g05540(**K**), and At3g26380 (**L**) was downregulated in both *adf4* and *ADF1-4Ri*. Standard

728 deviation of experimental triplicates is shown. Comparison with Col-0 was performed by
729 Student's *t*-test. Asterisks indicate that there is a significant difference (* $P<0.05$).
730 Representative data of biological triplicates are shown.
731